NATIONAL ADVISORY COMMITTEE FOR AERONAUTICS

REPORT No. 637

DETERMINATION OF BOUNDARY-LAYER TRANSITION ON THREE SYMMETRICAL AIRFOILS IN THE N. A. C. A. FULL-SCALE WIND TUNNEL

By ABE SILVERSTEIN and JOHN V. BECKER

1939

For sale by the Superintendent of Documents, Washington, D. C. - - - - - - - - - - - - - - Price 10 cents
Subscription price, $3 per year

AERONAUTIC SYMBOLS

1. FUNDAMENTAL AND DERIVED UNITS

	Symbol	Metric		English	
		Unit	Abbreviation	Unit	Abbreviation
Length	l	meter	m	foot (or mile)	ft. (or mi.)
Time	t	second	s	second (or hour)	sec. (or hr.)
Force	F	weight of 1 kilogram	kg	weight of 1 pound	lb.
Power	P	horsepower (metric)		horsepower	hp.
Speed	V	kilometers per hour	k.p.h.	miles per hour	m.p.h.
		meters per second	m.p.s.	feet per second	f.p.s.

2. GENERAL SYMBOLS

W, Weight$=mg$

g, Standard acceleration of gravity$=9.80665$ m/s^2 or 32.1740 ft./sec.^{2}

m, Mass$=\frac{W}{g}$

I, Moment of inertia$=mk^2$. (Indicate axis of radius of gyration k by proper subscript.)

μ, Coefficient of viscosity

ν, Kinematic viscosity

ρ, Density (mass per unit volume)

Standard density of dry air, 0.12497 kg-m^{-4}-s^2 at 15° C. and 760 mm; or 0.002378 lb.-ft.$^{-4}$ sec.^{2}

Specific weight of "standard" air, 1.2255 kg/m^3 or 0.07651 lb./cu. ft.

3. AERODYNAMIC SYMBOLS

S, Area

S_w, Area of wing

G, Gap

b, Span

c, Chord

$\frac{b^2}{S}$, Aspect ratio

V, True air speed

q, Dynamic pressure$=\frac{1}{2}\rho V^2$

L, Lift, absolute coefficient $C_L=\frac{L}{qS}$

D, Drag, absolute coefficient $C_D=\frac{D}{qS}$

D_0, Profile drag, absolute coefficient $C_{D_0}=\frac{D_0}{qS}$

D_i, Induced drag, absolute coefficient $C_{D_i}=\frac{D_i}{qS}$

D_p, Parasite drag, absolute coefficient $C_{D_p}=\frac{D_p}{qS}$

C, Cross-wind force, absolute coefficient $C_C=\frac{C}{qS}$

R, Resultant force

i_w, Angle of setting of wings (relative to thrust line)

i_t, Angle of stabilizer setting (relative to thrust line)

Q, Resultant moment

Ω, Resultant angular velocity

$\rho\frac{Vl}{\mu}$, Reynolds Number, where l is a linear dimension (e.g., for a model airfoil 3 in. chord, 100 m.p.h. normal pressure at 15° C., the corresponding number is 234,000; or for a model of 10 cm chord, 40 m.p.s., the corresponding number is 274,000)

C_p, Center-of-pressure coefficient (ratio of distance of c.p. from leading edge to chord length)

α, Angle of attack

ϵ, Angle of downwash

α_0, Angle of attack, infinite aspect ratio

α_i, Angle of attack, induced

α_a, Angle of attack, absolute (measured from zero-lift position)

γ, Flight-path angle

REPORT No. 637

DETERMINATION OF BOUNDARY-LAYER TRANSITION ON THREE SYMMETRICAL AIRFOILS IN THE N. A. C. A. FULL-SCALE WIND TUNNEL

By ABE SILVERSTEIN and JOHN V. BECKER

Langley Memorial Aeronautical Laboratory

80294—39——1

NATIONAL ADVISORY COMMITTEE FOR AERONAUTICS

HEADQUARTERS, NAVY BUILDING, WASHINGTON, D. C.

LABORATORIES, LANGLEY FIELD, VA.

Created by act of Congress approved March 3, 1915, for the supervision and direction of the scientific study of the problems of flight (U. S. Code, Title 50, Sec. 151). Its membership was increased to 15 by act approved March 2, 1929. The members are appointed by the President, and serve as such without compensation.

TECHNICAL COMMITTEES

AERODYNAMICS
POWER PLANTS FOR AIRCRAFT
AIRCRAFT MATERIALS
AIRCRAFT STRUCTURES
AIRCRAFT ACCIDENTS
INVENTIONS AND DESIGNS

Coordination of Research Needs of Military and Civil Aviation

Preparation of Research Programs

Allocation of Problems

Prevention of Duplication

Consideration of Inventions

LANGLEY MEMORIAL AERONAUTICAL LABORATORY

LANGLEY FIELD, VA.

Unified conduct, for all agencies, of scientific research on the fundamental problems of flight.

OFFICE OF AERONAUTICAL INTELLIGENCE

WASHINGTON, D. C.

Collection, classification, compilation, and dissemination of scientific and technical information on aeronautics.

REPORT No. 637

DETERMINATION OF BOUNDARY-LAYER TRANSITION ON THREE SYMMETRICAL AIRFOILS IN THE N. A. C. A. FULL-SCALE WIND TUNNEL

By Abe Silverstein and John V. Becker

SUMMARY

For the purpose of studying the transition from laminar to turbulent flow, boundary-layer measurements were made in the N. A. C. A. full-scale wind tunnel on three symmetrical airfoils of N. A. C. A. 0009, 0012, and 0018 sections. The effects of variations in lift coefficient, Reynolds Number, and airfoil thickness on transition were investigated. Air speed in the boundary layer was measured by total-head tubes and by hot wires; a comparison of transition as indicated by the two techniques was obtained.

The results indicate no unique value of Reynolds Number for the transition, whether the Reynolds Number is based upon the distance along the chord or upon the thickness of the boundary layer at the transition point. In general, the transition is not abrupt and occurs in a region that varies in length as a function of the test conditions. With increasing lift, the transition on the upper surface moves toward the forward stagnation point; whereas, on the lower surface, the transition progresses in the opposite direction. This effect is most marked for the thin airfoils. The total-head tubes and hot wires indicate essentially the same point of transition. Profile-drag results are given and a correlation of the drag and the transition measurements is attempted.

INTRODUCTION

The effect of skin friction on the air flow over a flat plate or an airfoil has been shown by many early writers to be restricted to a thin layer of air of reduced momentum that flows along the surface. The air flow in this boundary layer is laminar at low Reynolds Numbers; transition to a turbulent regime is, however, generally observed to occur when the Reynolds Number is increased. Extensive investigations have not yet provided a means for reliable prediction of the transition, although Burgers (reference 1), van der Hegge Zijnen (reference 2), Dryden (reference 3), Jones (reference 4), and others have shown that transition depends upon initial stream turbulence, Reynolds Number, pressure gradient, curvature, and surface roughness.

Prediction of the transition is necessary in order to predict the drag because the skin friction occurring with a laminar boundary layer is less than with a turbulent one. No reliable extrapolation of wind-tunnel drag results to flight may be made until the effects of all the factors upon which transition depends may be explicitly stated.

Owing to the effects of air-stream turbulence, the interpretation of wind-tunnel transition data for application to flight conditions has been difficult. The possibility of a direct comparison between wind-tunnel and flight results is provided by the equipment of the N. A. C. A. full-scale wind tunnel. The turbulence in the full-scale tunnel as indicated by sphere tests (reference 5) is 0.3 percent. The present investigation, which was made in the full-scale tunnel, is the first part of a program planned to correlate the flight and tunnel results.

In the tests, boundary-layer velocities were measured on the upper surfaces of airfoils of the N. A. C. A. 0009, 0012, and 0018 sections at tunnel velocities from 30 to 90 miles per hour (values of the Reynolds Number from 1,730,000 to 5,020,000) over a lift-coefficient range from −0.57 to 0.65. The tests were made with rectangular 6- by 36-foot metal airfoils having aerodynamically smooth surfaces. Measurements of profile drag at zero lift by means of force tests and the momentum method were also obtained.

In order to aid in the presentation of the experimental data and to clarify discussion, the following arbitrary definitions have been adopted for the present paper.

The transition region is the region in which the boundary-layer flow changes from laminar to turbulent. The beginning of this region will be referred to as the "transition point" and will be considered to be the point at which the velocity near the surface begins to show an abnormal increase. The end of the transition region has been taken as the point at which the velocity near the surface has reached a maximum.

SYMBOLS

The symbols used herein are defined as follows:

c_l, section lift coefficient.
C_{D_0}, profile-drag coefficient of the wing.
c_{d_0}, section profile-drag coefficient.
C_f, skin-friction coefficient.
u, local velocity, f. p. s.
U, velocity at edge of boundary layer, f. p. s.
V, tunnel air speed, m. p. h.
y, distance above airfoil surface.
s, distance along airfoil surface from forward stagnation point.
c, wing chord.
t, wing thickness.
δ, boundary-layer thickness ($u \cong 0.99U$ at δ).
δ^*, displacement thickness of the boundary layer

$$\left(\delta^* = \frac{1}{U}\int_0^{\delta}(U-u)dy\right)$$

R_δ, Reynolds Number based on the boundary-layer thickness at transition (based on U).
R_x, Reynolds Number based on the chordwise distance from the forward stagnation point to the transition point (based on V).
p, local pressure.
q, dynamic pressure, $\frac{1}{2}\rho V^2$.

METHODS AND APPARATUS

In a paper on boundary-layer transition in flight, Jones (reference 4) has given an excellent discussion of the methods by which the transition on an airfoil may be detected. Briefly, the transition may be determined either from observations of the velocity at the airfoil surface by means of a single total-head tube or a hot wire or from velocity measurements at several distances from the surface so that the boundary-layer profile may be defined. When the indicated velocity at the airfoil surface shows a marked increase in the transition region, the single-tube or the hot-wire method is quite satisfactory as a transition indicator. If, however, the chordwise velocity gradient in the boundary layer is low, so that the point of minimum velocity is indeterminate, the more extensive measurements of the velocity profiles are more dependable.

Characteristic velocity profiles for the laminar and turbulent boundary layers are shown in figure 1. Representative data showing the velocity changes that occur at transition for several heights in the boundary layer are shown in figure 2 to illustrate the fact that no sharp indication of transition is given for some heights in the boundary layer. It will be noted (fig. 2) that the transition point is shown to occur at $s/c = 0.26$ for all the heights except 0.050 inch; this height is about that at which the laminar and turbulent profiles intersect, as shown in figure 1, and no extreme velocity gradients are therefore expected.

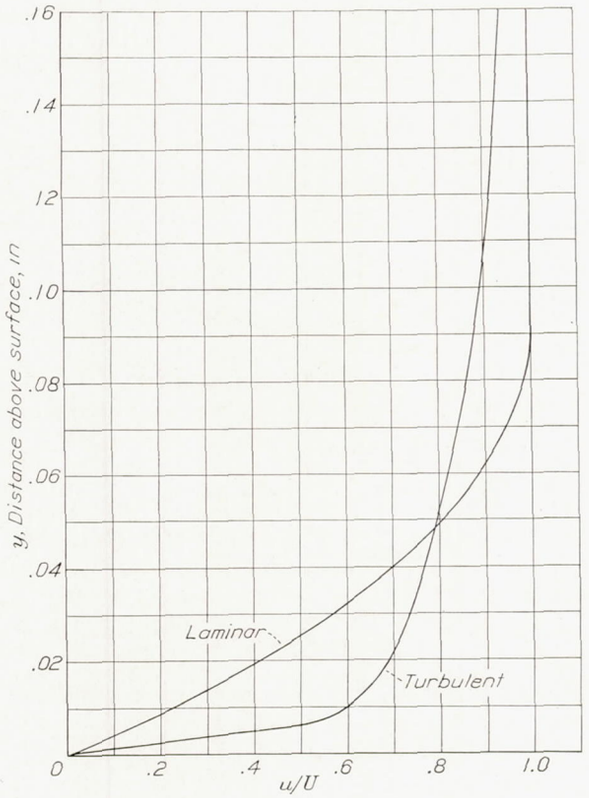

FIGURE 1.—Typical laminar and turbulent boundary-layer velocity profiles.

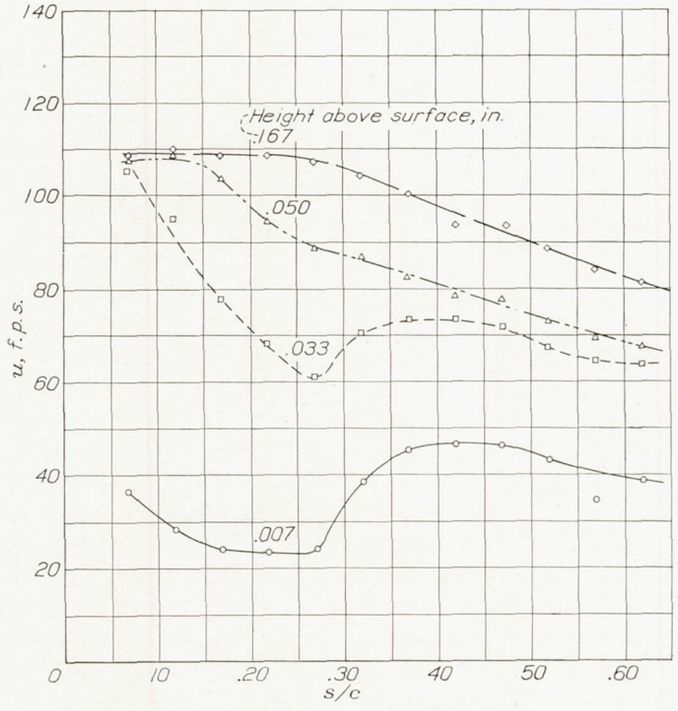

FIGURE 2.—Variation in the velocity of the boundary layer of the N. A. C. A. 0012 airfoil at several heights above the surface.

Hot-wire method.—The velocities in the boundary layer 0.01 inch above the wing surface were measured,

as suggested by Dr. H. L. Dryden, by means of platinum hot wires 0.001 inch in diameter and 1 inch long (fig. 3). The platinum wires were soldered across the ends of forks of B. & S. gage 26 (0.0159 inch) enameled copper wire. The ends of the forks were filed to thicknesses of 0.010 inch and sprung to keep the hot wire

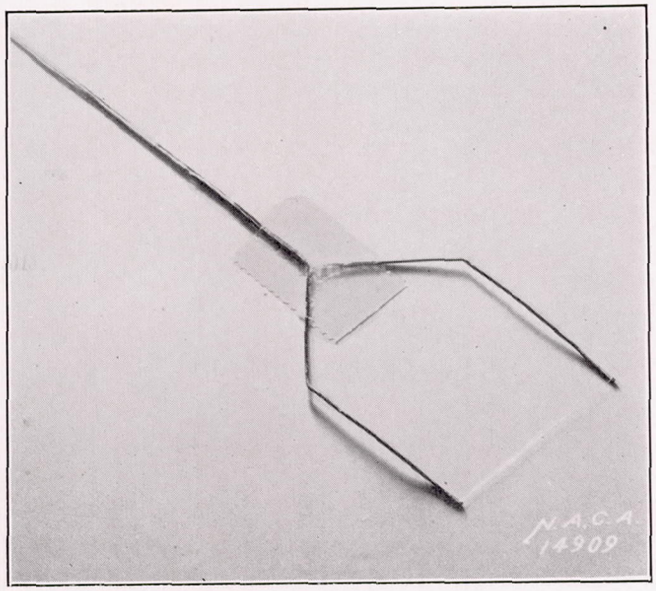

FIGURE 3.—Hot wire mounted on the airfoil. The platinum wire is 0.001 inch in diameter, 1 inch long, and 0.01 inch above the surface.

taut at all temperatures. The enameled wires were cemented together with an insulating glue at the base of the forks. In order to reduce the time required for obtaining the data, 12 hot-wire units were arranged on the wing at 0.05c intervals between the 0.10c and the 0.70c positions, as shown in figure 4. The wires were spaced at sufficient distances along the span so that the wake of one wire did not pass over another. They could be switched into the measuring circuit one at a time.

A Wheatstone bridge circuit, with a hot wire as one arm of the bridge, was used to maintain the resistance of the wire at a constant value (fig. 4). The resistances AB and BC were made large so that the current to the hot wire would be about equal that in the battery circuit. A 5-ohm rheostat was used to balance the bridge for the initial still-air condition; an initial current of 0.15 ampere in the battery circuit corresponded to a wire temperature of 150° C. The ½-ohm rheostat in series with each hot wire was used to adjust the resistances of the 12 circuits to precisely the same value after installation on the wing. Adjustment of a 50-ohm rheostat in the battery circuit was used to increase the current through the hot wire as the air speed was increased. During the tests, the procedure was to switch in a hot wire by means of the multiple switch, to adjust resistance AE until the galvanometer read zero, and then to observe the reading of the ammeter.

In order to obtain satisfactory velocity readings, it was necessary to calibrate the hot wire on a flat plate against a total-head tube at the same effective height. Velocity indications based on a calibration in a free stream in which the heat-loss and interference effects are neglected give completely erroneous results.

Total-head-tube method.—The velocities at four heights above the surface were measured by a bank of four small total-head tubes and a single static tube (figs. 5 and 6). (The static pressure in the boundary layer has been shown to be constant.) The tubes are of stainless steel, 0.040-inch outside diameter, with a 0.003-inch wall thickness. The measuring ends of the total-head tubes were flattened to an outside thickness of 0.012 inch for a length of 1 inch from the opening. A hemispherical plug was inserted in the end of the static-pressure tube and four 0.005-inch holes, equally spaced, were drilled around the circumference. The tubes were 3⅛ inches long and were soldered into 1/16-inch copper tubes, which extended back along the chord of the airfoil to rubber tubing that was led along the trailing edge of the airfoil to manometers. Required height adjustment was secured by placing a ⅛-inch

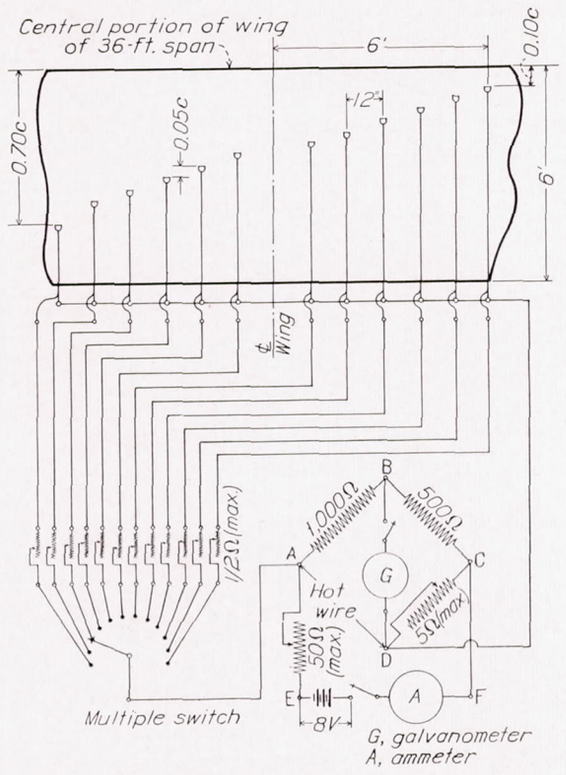

FIGURE 4.—Location of 12 hot-wire units on the 6- by 36-foot airfoil, and wiring diagram of Wheatstone bridge circuit.

bridge 3¼ inches back from the tube ends and bending the tubes at this bridge to conform to an accurate templet-type gage. The tubes showed no tendency to lose adjustment during a run and observations during the tests indicated that no vibration of the tubes occurred.

Calibration of the bank of static and total-head tubes in a uniform stream against a standard pitot-static tube indicated that they were accurate to within 1 percent.

When the results obtained with the total-head tubes were plotted, it was necessary to correct the geometric height of the tube centers to an effective

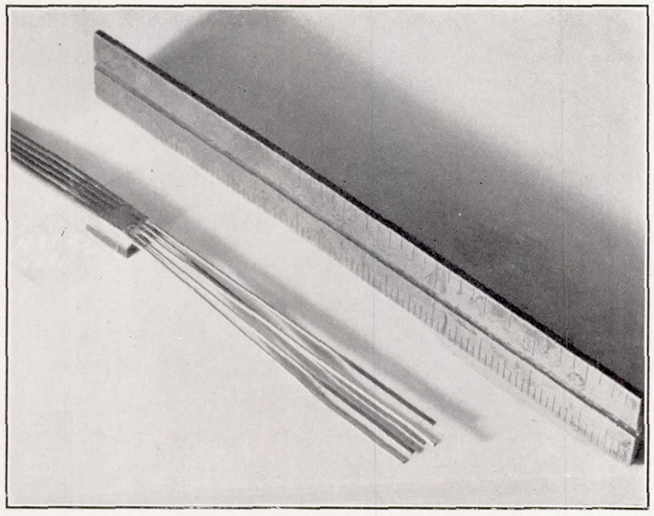

FIGURE 5.—Bank of total-head tubes and static tube mounted on the airfoil.

height to take into account the velocity gradient in the boundary layer. The effective dynamic pressure over the tube opening is greater than the pressure at the center of the tube. The effective height was obtained on the assumption of a linear velocity gradient.

Airfoils.—The three metal airfoils used in the tests were constructed with the utmost precision so that the section profiles and the surfaces were as fair and smooth as possible. After the metal surfaces had been filed to templet dimensions, they were alternately filled with a standard metal primer and rubbed with fine-grade water sandpaper until they were considered to be aerodynamically smooth; they were then waxed and polished. Aerodynamic smoothness is herein defined as the smoothness after which further improvements do not decrease the skin friction. Information on wing smoothness obtained in previous investigations in the N. A. C. A. 8-foot high-speed wind tunnel served as a guide. The airfoils were carefully dusted before each series of tests.

TESTS

The hot wires were normally spaced at 0.05 c intervals from the 0.10 c to the 0.70 c station. For some of the tests, measurements were also obtained at the 0.05 c position. The air-flow velocities at 0.010 inch above the airfoil surface were measured at lift coefficients of −0.57, 0, 0.33, and 0.65 and at tunnel speeds of about 30, 45, 60, 75, and 90 miles per hour.

In the tests using the total-head tubes, the velocities at effective heights of 0.007, 0.033, 0.050, and 0.167 inch above the wing surface were measured for lift coefficients of −0.57, 0, and 0.65 and at tunnel speeds of about 60 and 90 miles per hour. The measurements were taken at 0.05 c intervals from the 0.10 c to the 0.70 c position.

Profile-drag measurements were obtained at zero lift for all the airfoils over a range of test velocities.

Additional tests were made on the N. A. C. A. 0012 airfoil to determine the effect on transition and drag of a small protuberance across the span near the leading edge. Narrow gummed tapes 0.003, 0.006, and 0.009 inch thick were attached one at a time across the span of the airfoil at the 0.05c position on the upper surface. The velocities were measured by the hot-wire method at an angle of attack of 0° and a tunnel speed of 75 miles per hour. Drag measurements were also made for these three runs.

RESULTS AND DISCUSSION

The boundary-layer measurements obtained by the hot-wire method are shown in figures 7, 8, and 9 for the N. A. C. A. 0008, the N. A. C. A. 0012, and the N. A. C. A. 0018 airfoils, respectively, at several section lift coefficients. Figures 10, 11, and 12 show corresponding results obtained with the total-head tubes on the wing surface. The forward stagnation point, from which s was measured, was obtained from theoretical pressure-distribution calculations. The section lift coefficients c_l were computed from the curves of theoretical span load distribution and from the measured lift

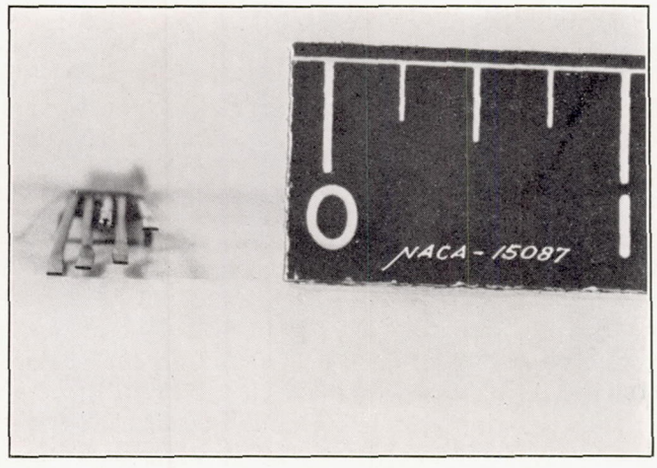

FIGURE 6.—Boundary-layer survey tubes in front view. The effective heights of the openings above the surface are 0.007 inch, 0.033 inch, 0.050 inch, and 0.167 inch. The height of the static tube is 0.175 inch.

on the wings. The boundary-layer velocity profiles, measured with the bank of total-head tubes, are shown in figures 13, 14, and 15 for the three airfoils at several section lift coefficients and positions along the airfoil surface. Boundary-layer velocity profiles for the transition region are plotted in a nondimensional form in figures 16, 17, and 18.

Comparison of methods for detecting transition.—An analysis of the results in figures 7 to 12 shows that the surface total-head tube or the hot wire is adequate to indicate the transition point except for cases in which the downstream velocity gradient at the airfoil surface is so small that the point of minimum velocity is not clearly defined. This condition occurs on the upper surface of the airfoils at negative lift coefficients (corresponding to the lower surface of the airfoils at positive lift coefficients), in which case the transition point is indicated as far back as 50 to 60 percent of the chord. The nondimensional boundary-layer profiles for the negative lift coefficients (figs. 16 (a), 17 (a), and 18 (a)) are of considerable aid in investigation of the transition for these cases. The shape of the profiles in the transition region is apparently a function of the length of the region and, at negative lift coefficients, the ⅐-horsepower turbulent profiles did not occur until 20 to 30 percent of the chord behind the transition point.

The transitions as indicated by the hot wires and the surface tube show a reasonable agreement with the maximum variation of the indications usually not in excess of 3 percent of the chord. The hot-wire measurements indicated the transition region by large fluctuations in the current required to balance the bridge. These fluctuations began slightly before the transition point and continued through the transition region, reaching maximum intensity at about the transition point. Owing to the heavy damping in the long pressure leads to the total-head tubes, the actual violence of these fluctuations was not observed; however, there was a distinct indication of unsteadiness in the readings at the transition point.

The hot-wire method as used in the present tests was considerably faster than the total-head method, inasmuch as it was possible to obtain results from each of the 12 wires on the wing without a change in the set-up. The readings were also obtained much more rapidly because from 3 to 4 minutes were required for the readings from the pressure tubing to reach equilibrium. The observations obtained with the total-head tubes seemed somewhat more consistent, however, and a smaller scatter of the experimental points occurred.

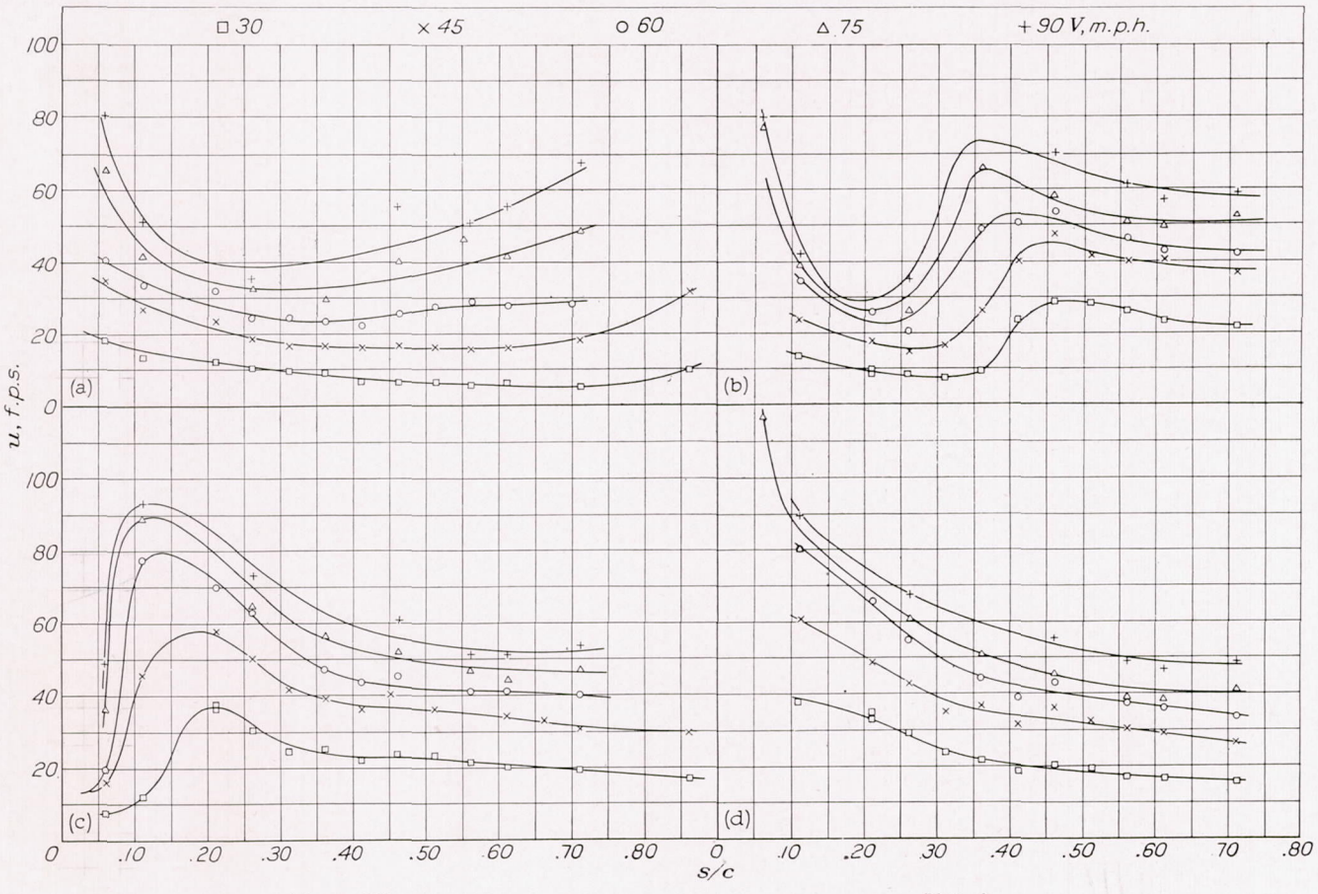

(a) $c_l = -0.57$.
(b) $c_l = 0$.
(c) $c_l = 0.33$.
(d) $c_l = 0.65$.

FIGURE 7.—Hot-wire measurements of the boundary-layer velocities 0.010 inch above the surface of the N. A. C. A. 0009 airfoil.

Effect of lift on transition.—The effect of variations in the section lift coefficient on the transition point for various Reynolds Numbers is shown in figures 19, 20, and 21. The results from the surface total-head tubes and the hot wires for zero and positive lift coefficients are included. The transition points were estimated for $c_l = -0.57$ from the boundary-layer profiles of figures 16 (a), 17 (a), and 18 (a).

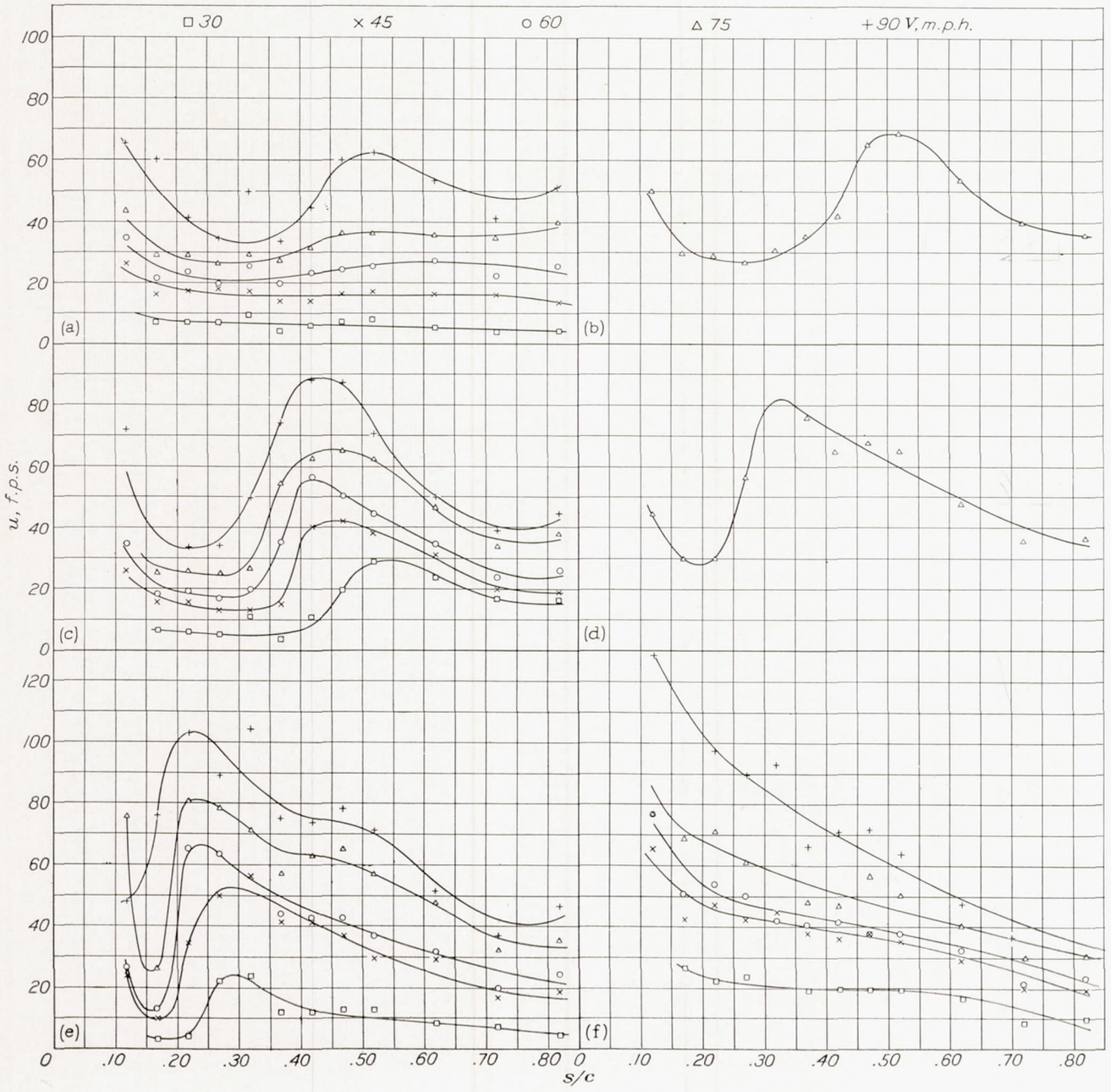

(a) $c_l = -0.57$.
(b) $c_l = -0.16$.
(c) $c_l = 0$.
(d) $c_l = 0.16$.
(e) $c_l = 0.33$.
(f) $c_l = 0.65$.

FIGURE 8.—Hot-wire measurements of the boundary-layer velocities 0.010 inch above the surface of the N. A. C. A. 0012 airfoil.

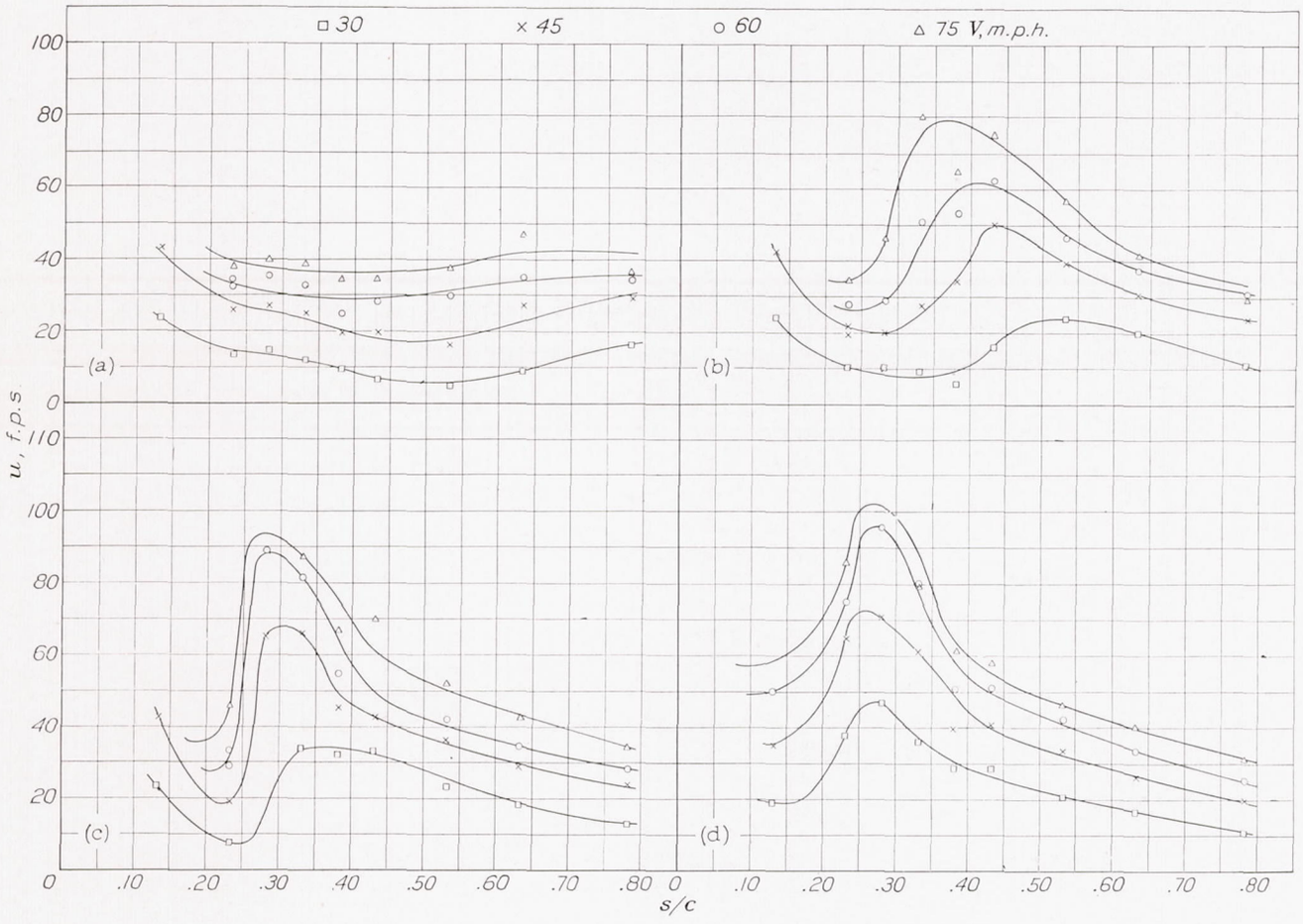

(a) $c_l = -0.57$.
(b $c_l = 0$.
(c) $c_l = 0.33$.
(d) $c^l = 0.65$.

FIGURE 9.—Hot-wire measurements of the boundary-layer velocities 0.010 inch above the surface of the N. A. C. A. 0018 airfoil.

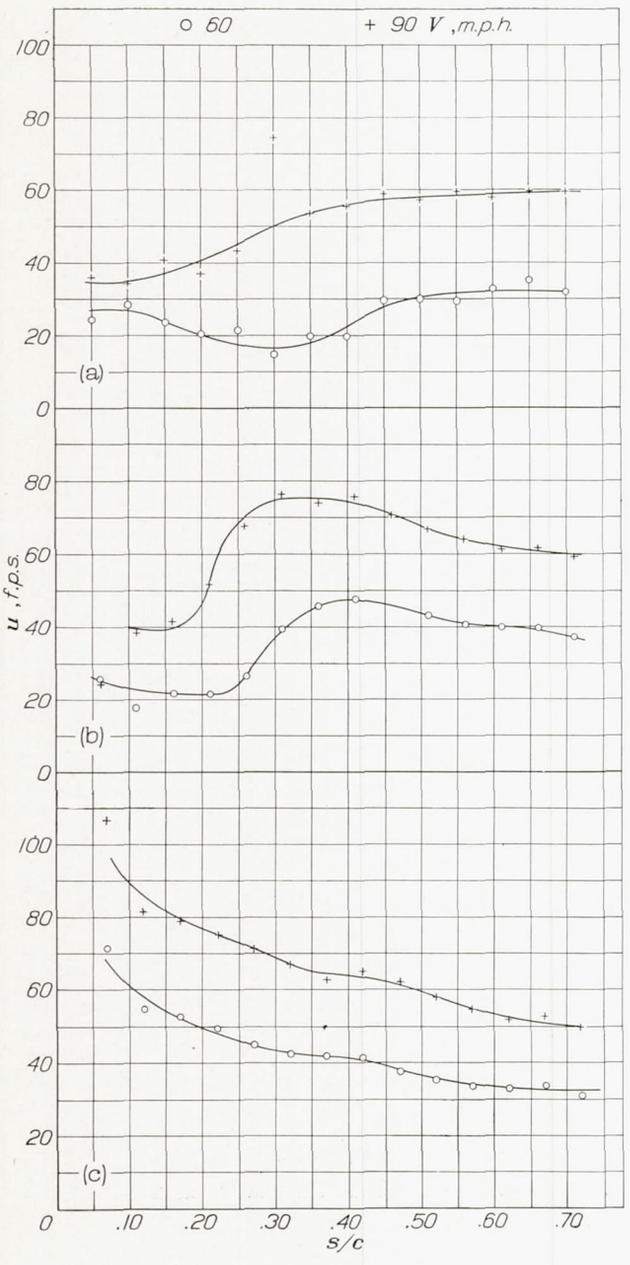

(a) $c_l = -0.57$.
(b) $c_l = 0$.
(c) $c_l = 0.65$.

FIGURE 10.—Total-head-tube measurements of boundary-layer velocities on the surface of the N. A. C. A. 0009 airfoil.

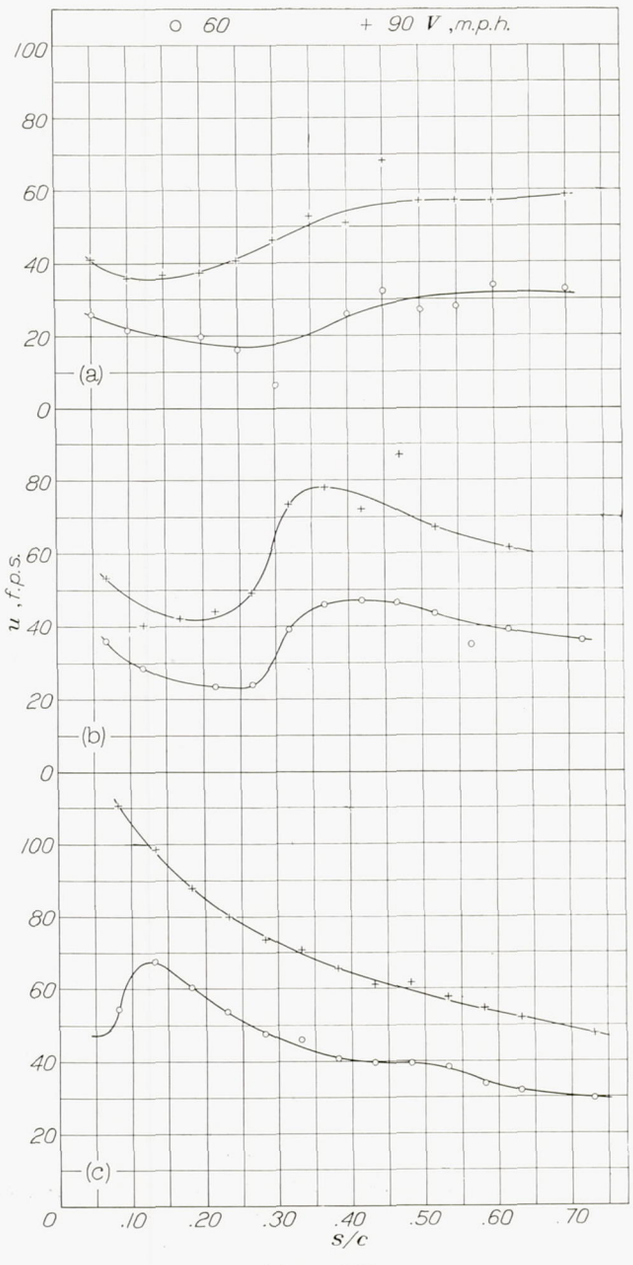

(a) $c_l = -0.57$.
(b) $c_l = 0$.
(c) $c_l = 0.65$.

FIGURE 11.—Total-head-tube measurements of boundary-layer velocities on the surface of the N. A. C. A. 0012 airfoil.

The results show that the transition point on the upper surface moves toward the forward stagnation point with increasing lift coefficient, the rate of forward motion increasing with decreasing wing thickness. This phenomenon may be correlated with pressure-distribution measurements, which are shown in figures 22, 23, and 24, for the airfoils tested; it will be noted that the adverse pressure gradient over the forward part of the airfoil varies in the same manner. The pressure distribution for zero lift as measured with the static tube at the surface and the theoretically predicted pressure distribution are in good agreement (figs. 22, 23, and 24).

Effect of Reynolds Number on transition.—The effect of variation in the Reynolds Number on the position of the transition point and the end of the transition region is shown in figure 25 for section lift coefficients c_l of 0 and 0.33. The variation in the transition point for other lift coefficients may be noted by a visual cross plot of figures 19, 20, and 21. The transition point moves forward with increasing Reynolds Number at a rate that is not greatly different for the 9, 12, or 18 percent thick wing. Transition occurred at no unique value of R_x but varied at $c_l=0$ from approximately 500,000 to 1,100,000. At $c_l=-0.57$, a value of R_x of over 2,500,000 was reached before transition. The transition Reynolds Number increases with increasing wing Reynolds Number. The R_δ values at the transition point (Reynolds Numbers based on the boundary-layer thickness at transition) vary from about 3,000 to 6,000 at zero lift and show no consistent change with wing Reynolds Number.

The considerable scatter in the experimentally measured positions of the end of the transition region (fig. 25) prevents definite conclusions from being drawn as to the effect of Reynolds Number on the width of the transition region. In general, however, the width did not appear to vary markedly with the Reynolds Number for any of the wing lift coefficients investigated.

Effect of airfoil thickness on transition.—The effect of variation in the wing thickness on the location of the transition point is summarized in figure 26. The points were obtained from cross-plotting the faired curves of figures 19, 20, and 21. Results are given for two tunnel speeds corresponding to Reynolds Numbers of about 3,350,000 and 5,020,000.

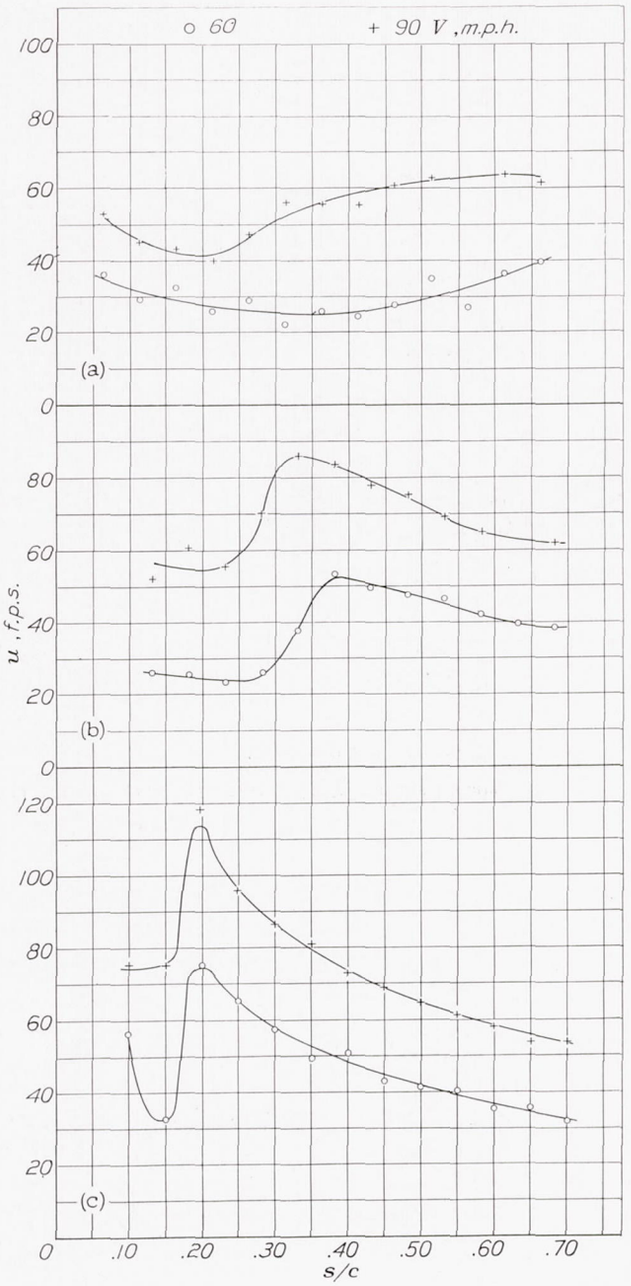

(a) $c_l=-0.57$.
(b) $c_l=0$.
(c) $c_l=0.65$.

FIGURE 12.—Total-head-tube measurements of boundary-layer velocities on the surface of the N. A. C. A. 0018 airfoil.

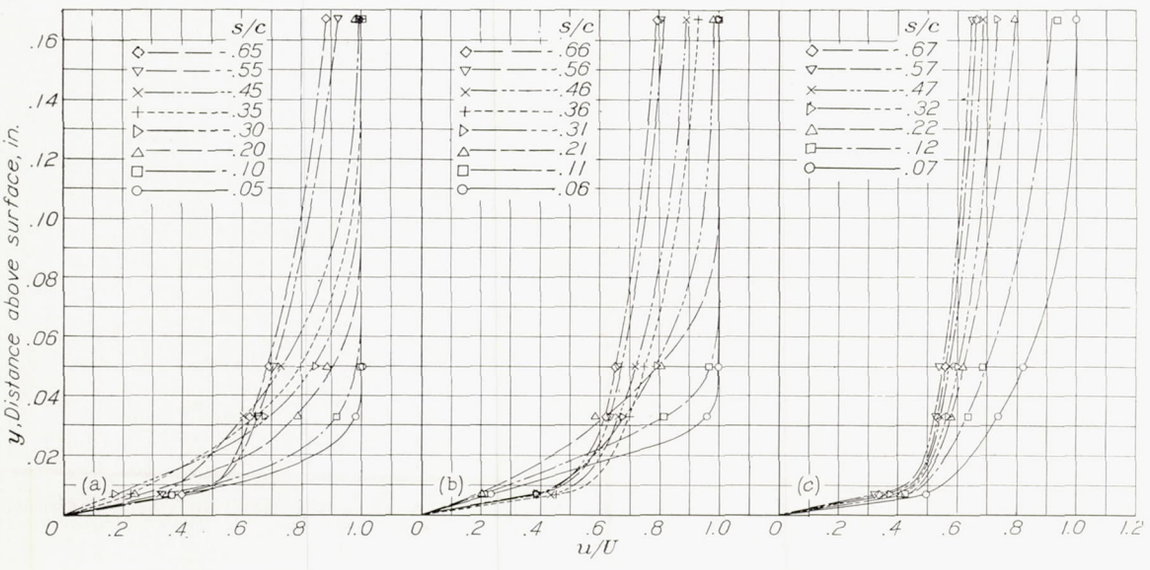

(a) $c_l = -0.57$. (b) $c_l = 0$. (c) $c_l = 0.65$.

FIGURE 13.—Boundary-layer velocity profiles at several chord positions on the N. A. C. A. 0009 airfoil. Tunnel air speed, 60 m. p. h.

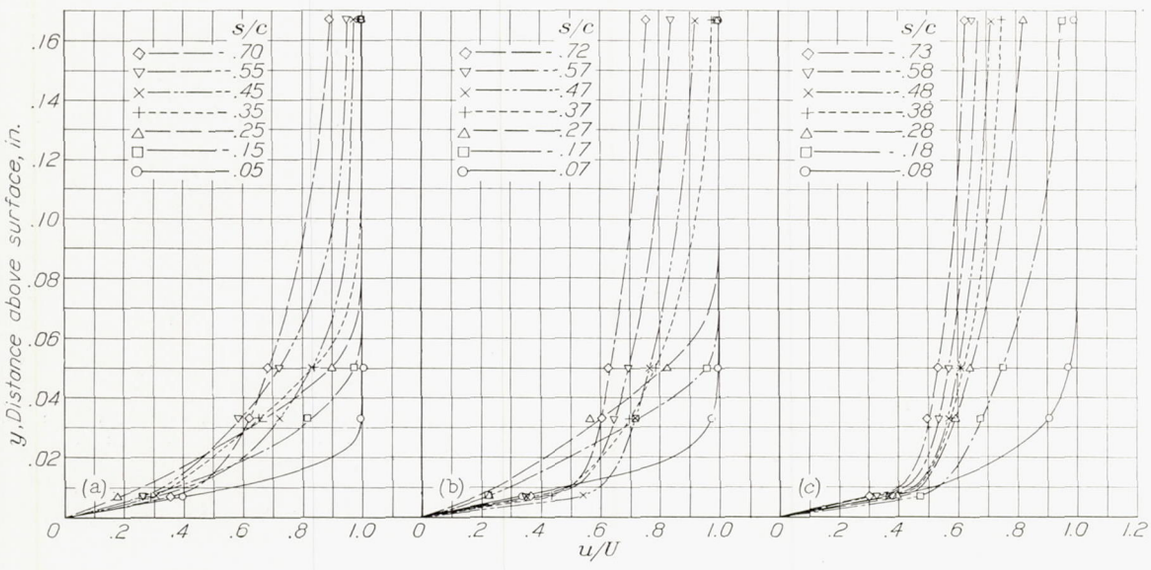

(a) $c_l = -0.57$. (b) $c_l = 0$. (c) $c_l = 0.65$.

FIGURE 14.—Boundary-layer velocity profiles at several chord positions on the N. A. C. A. 0012 airfoil. Tunnel air speed, 60 m. p. h.

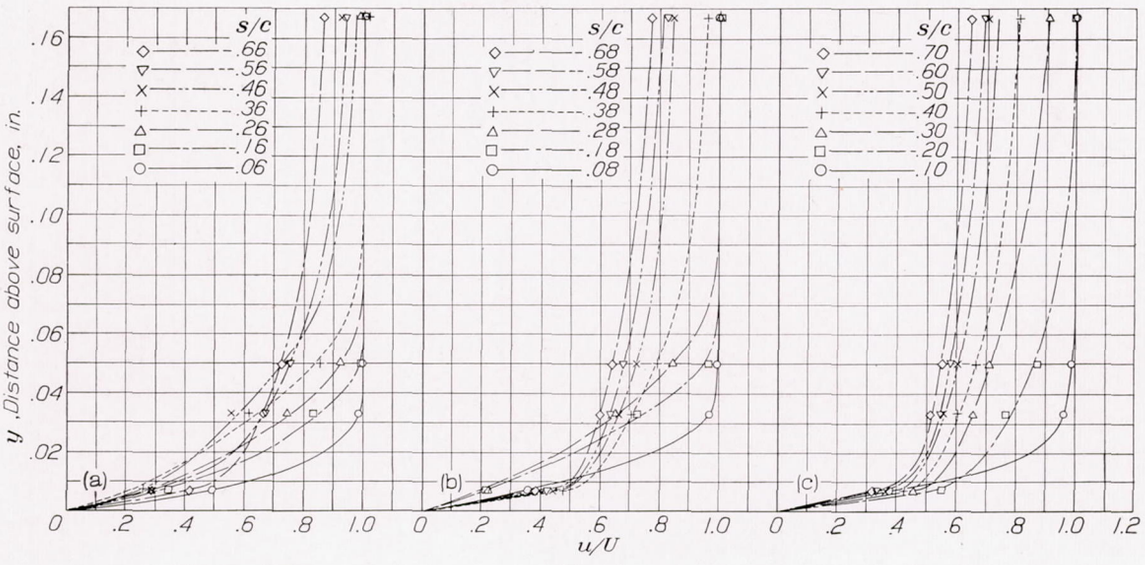

(a) $c_l = -0.57$. (b) $c_l = 0$. (c) $c_l = 0.65$.

FIGURE 15.—Boundary-layer velocity profiles at several chord positions on the N. A. C. A. 0018 airfoil. Tunnel air speed, 60 m. p. h.

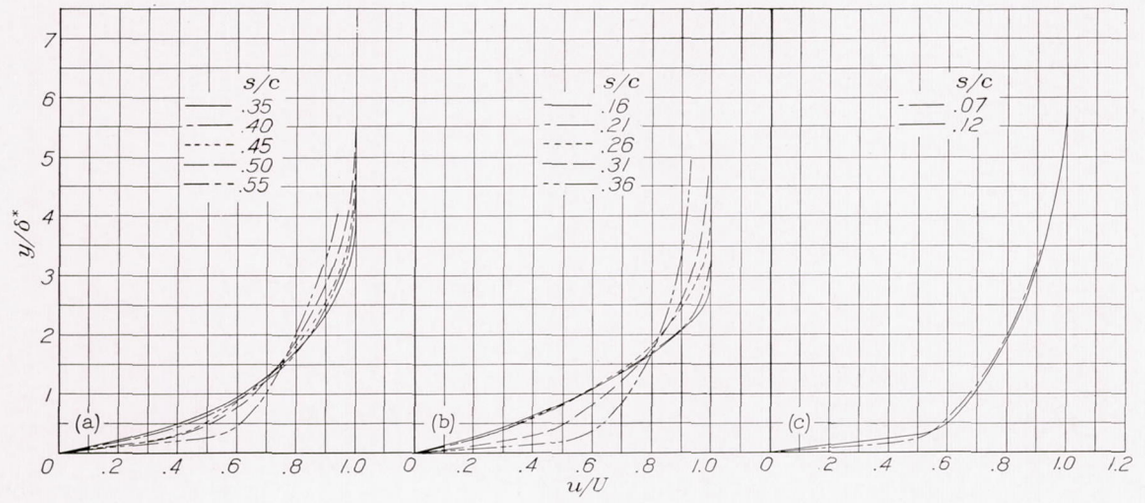

(a) $c_l = -0.57$. (b) $c_l = 0$. (c) $c_l = 0.65$.

FIGURE 16.—Nondimensional boundary-layer velocity profiles in the transition region for the N. A. C. A. 0009 airfoil. Tunnel air speed, 60 m. p. h.

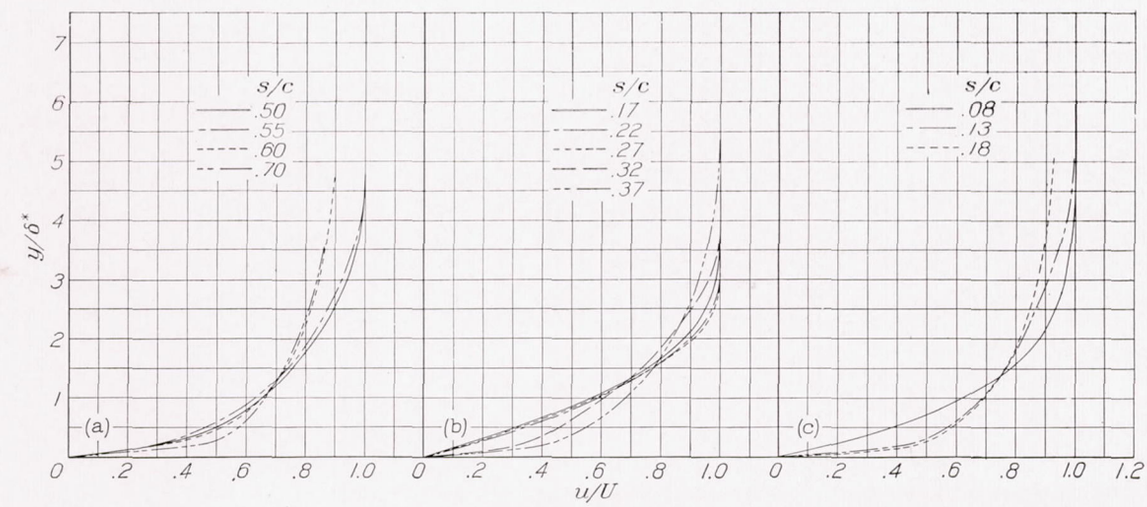

(a) $c_l = -0.57$. (b) $c_l = 0$. (c) $c_l = 0..65$

FIGURE 17.—Nondimensional boundary-layer velocity profiles in the transition region for the N. A. C. A. 0012 airfoil. Tunnel air speed, 60 m. p. h.

At $c_l=0$ and 0.33, the transition point occurred at the same chord position for the $0.12c$ and the $0.18c$ thick wing; however, it occurred considerably closer to the stagnation point for the $0.09c$ airfoil. At $c_l=0.65$, the transition point moved rearward with increasing thickness in an almost linear manner. The later transition for the thicker airfoils is directly related to the more favorable pressure distribution over the surface, as previously mentioned.

It is of interest to note that the pressure gradients over the symmetrical airfoils are not so favorable to late transitions as those over conventional cambered airfoils, and it may be expected that the transition will occur farther back along the chord for a cambered airfoil. The later transitions indicated in flight in reference 4 may be due in part to the more favorable pressure gradients, as is shown by a comparison of the pressure-distribution curves of reference 4 with those for the symmetrical airfoils (figs. 22, 23, and 24).

almost at the airfoil nose. These results are in agreement with previous studies showing the effects of rivets and surface irregularities and reemphasize the importance of smooth wing surfaces for low drag.

Correlation of profile drag and transition point.—The section profile-drag measurements for the symmetrical airfoils at zero lift are given in figure 28 for the range of test Reynolds Numbers. The profile-drag coefficients were obtained by both force and momentum measurements that were in excellent agreement (reference 6). Inasmuch as the knowledge of the transition point is of particular interest as an aid in the estimation of the profile drag, an attempt has been made to correlate the transition measurements with the observed profile-drag measurements for the representative case of the N. A. C. A. 0009 airfoil at zero lift. The thinnest airfoil was chosen to avoid a large pressure drag. At a Reynolds Number of 3,350,000, the transition point occurs at $s/c=0.23$ and the transition region extends

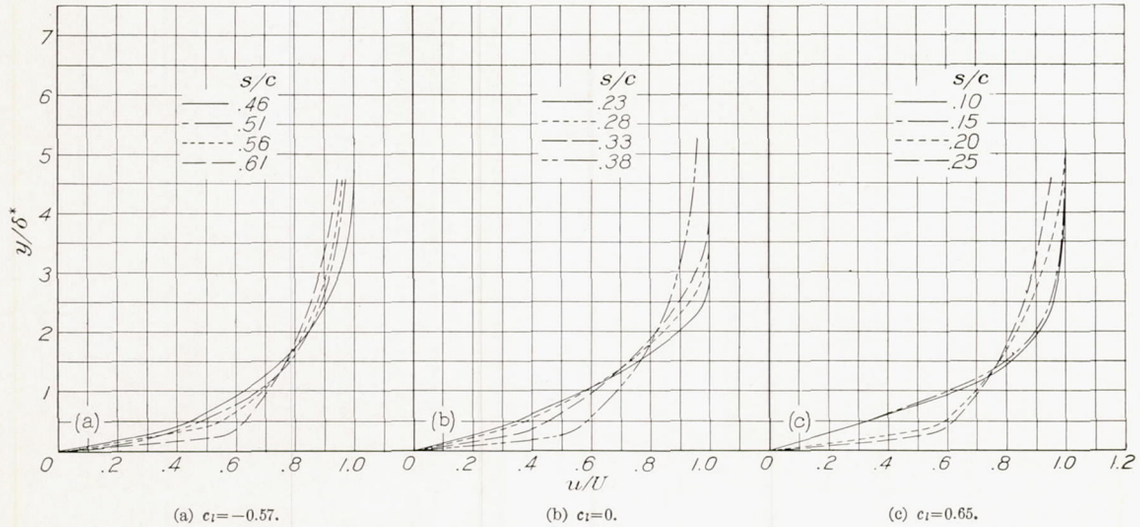

(a) $c_l=-0.57$. (b) $c_l=0$. (c) $c_l=0.65$.

FIGURE 18.—Nondimensional boundary-layer velocity profiles in the transition region for the N. A. C. A. 0018 airfoil. Tunnel air speed, 60 m. p. h.

Effect of protuberances on transition.—The effect of a protuberance near the leading edge on transition and the increase in the drag above that of the aerodynamically smooth wing is shown in figure 27. The gummed tape 0.003 inch thick placed at the $0.05c$ station had a slight tendency to move the transition point forward and increased the drag about 2.3 percent. The 0.006-inch-thick tape moved the transition point forward only about 1 percent; however, it shortened the transition region to about 10 percent and added 3.7 percent drag. The 0.009-inch-thick tape moved the transition point ahead of the 10-percent-chord station and added 7.5 percent drag. The transition region in the case of the 0.009-inch tape was very long and extended to the $0.35c$ station.

No rational explanation of the effects observed when the tapes were used can be offered. It should be noted, however, that a protuberance with a height of less than 0.01 inch was sufficient to cause transition to occur from $s/c=0.23$ to 0.40 (fig. 10(b)). The section profile-drag coefficient c_{d_0} corresponding to these test conditions is 0.0061 (fig. 28).

For the laminar and transition regions, it was possible, inasmuch as the complete boundary-layer profiles had been measured, to determine the drag by integration of the loss in momentum by means of the von Kármán momentum equation, taking into account the pressure distribution over the surface. From this calculation it was found that the average skin-friction coefficient C_f over the laminar and transition region was 0.0026.

This skin-friction coefficient is based on an area of only 40 percent of the surface on one side of the airfoil. In order to convert C_f into the usual coefficient form c_{d_0}, the value is doubled and multiplied by 0.40 so that the contribution to c_{d_0} of the laminar and transition regions is 0.0021.

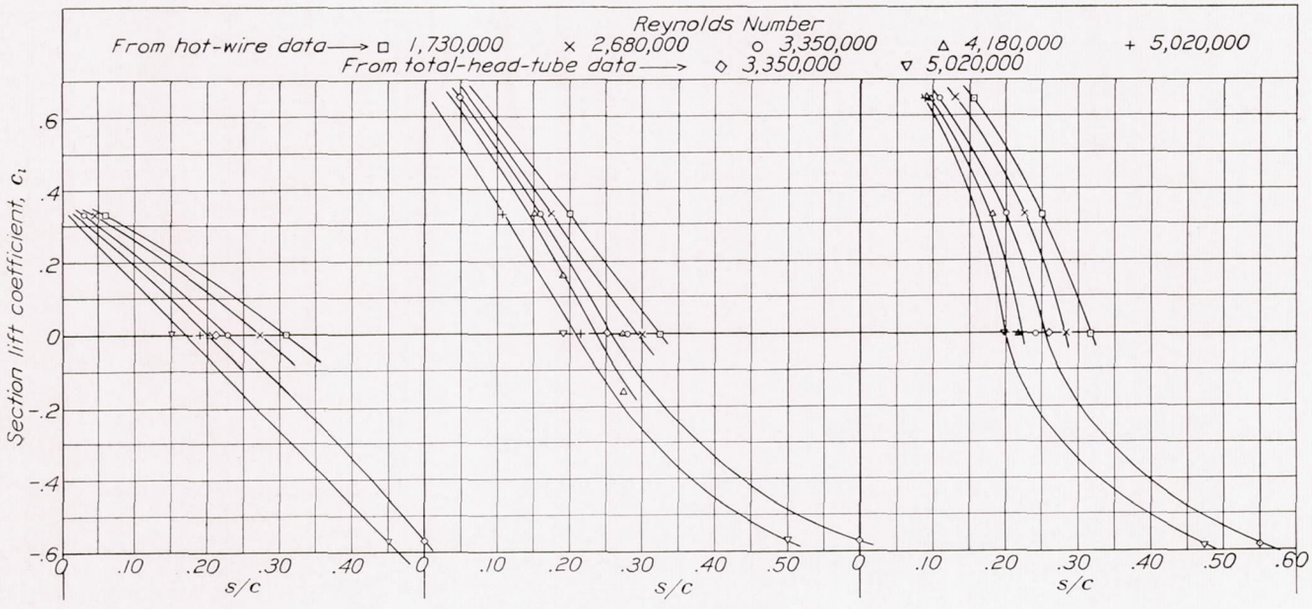

FIGURE 19.—N. A. C. A. 0009. FIGURE 20.—N. A. C. A. 0012. FIGURE 21.—N. A. C. A. 0018.

Variation of the transition point with section lift coefficient for the N. A. C. A. 0009, 0012, and 0018 airfoils.

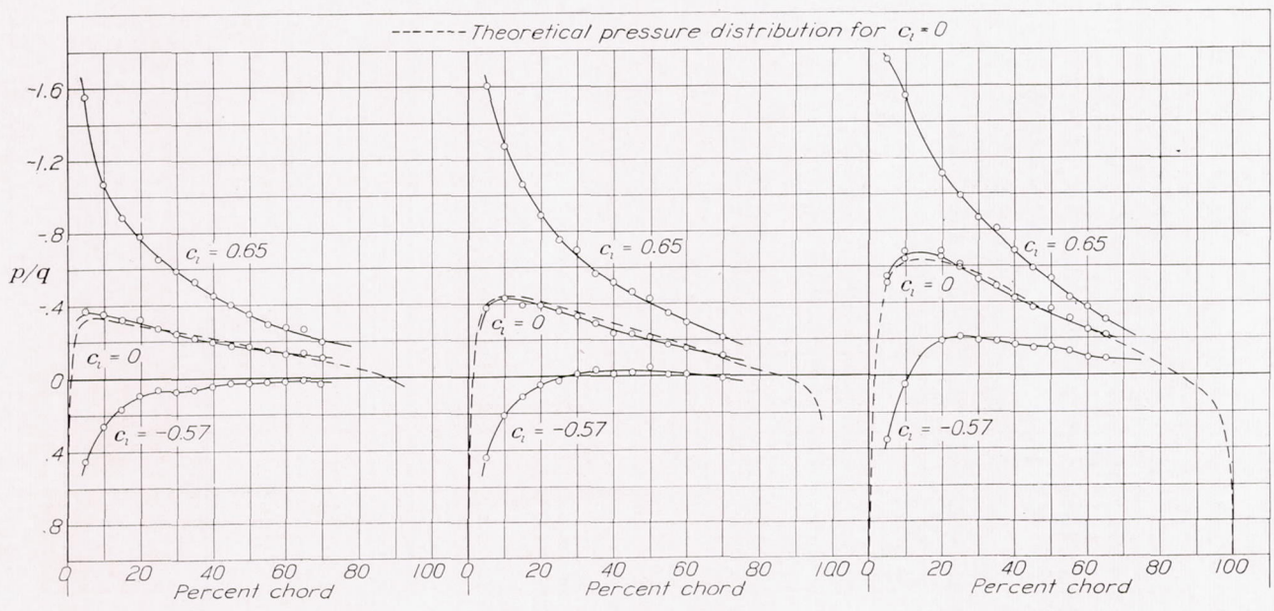

FIGURE 22.—N. A. C. A. 0009. FIGURE 23.—N. A. C. A. 0012. FIGURE 24.—N. A. C. A. 0018.

Pressure distribution on the upper surface of the N. A. C. A. 0009, 0012, and 0018 airfoils for three section lift coefficients.

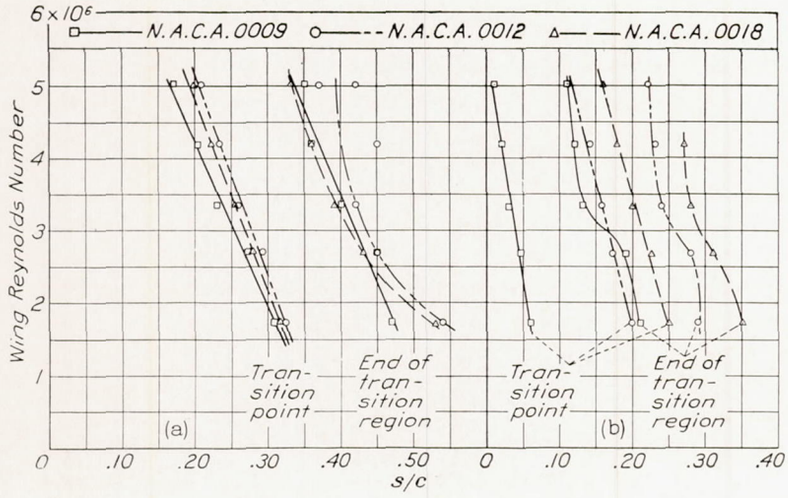

(a) $c_l=0$. (b) $c_l=0.33$.

FIGURE 25.—Effect of Reynolds Number on the transition point and extent of the transition region.

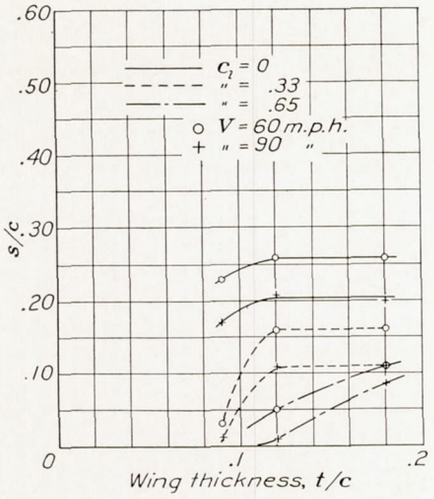

FIGURE 26.—Effect of airfoil thickness on the location of the transition point.

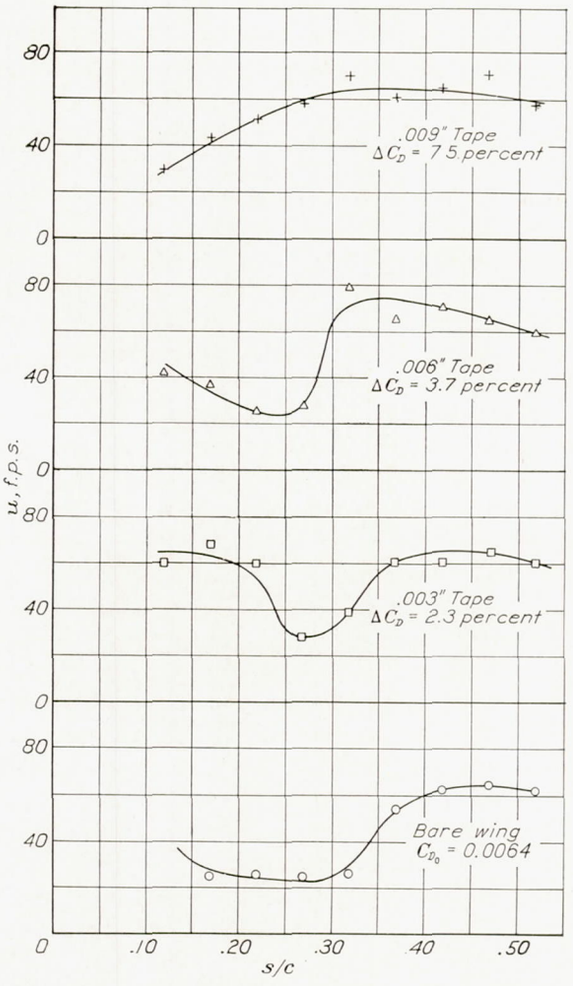

FIGURE 27.—Effect in the transition and drag of the N. A. C. A. 0012 airfoil of small protuberances at the 0.05c point on the upper surface. Reynolds Number=4,180,000.

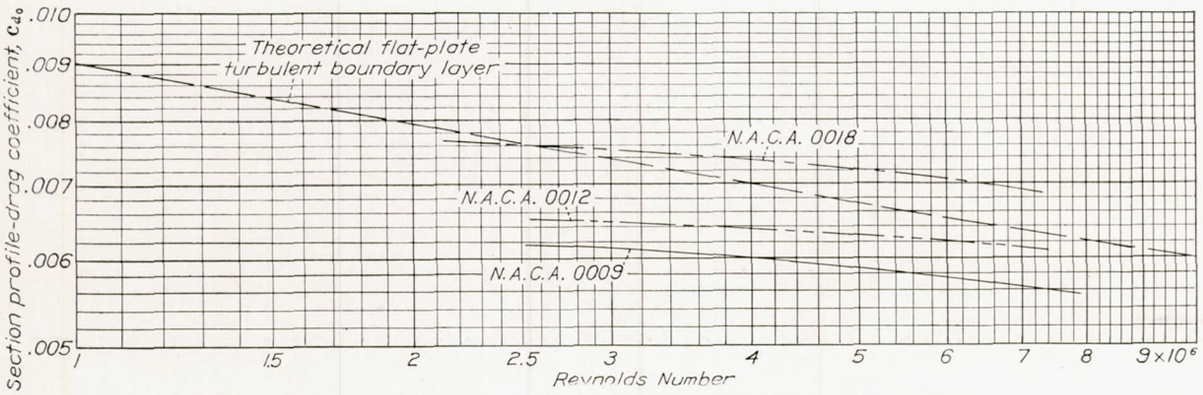

FIGURE 28.—Section profile-drag coefficients at zero lift for the N. A. C. A. 0009, 0012, and 0018 airfoils.

Complete turbulent profiles were not measured; the determination of the drag for the turbulent region therefore required the application of the empirical skin-friction laws derived for flat plates, suitably corrected by the method of Dryden and Kuethe (reference 7) for the pressure gradient on the airfoil. The crux of the whole calculation lies, however, in the assumption made regarding the state of development of the turbulent layer at the end of the transition region. If the drag for the turbulent region is computed according to the most obvious assumption, that the developed turbulent layer begins with a momentum loss equal to that at the end of the transition region, the value of the drag is much too high so that, when it is added to the drag for the laminar and transition regions, a negative pressure drag on the airfoil is indicated.

It is believed that further study of the local skin-friction coefficients in the boundary layer will be required in order to predict the wing profile drag, even when the transition point is known.

CONCLUDING REMARKS

The results of this investigation are consistent with those of previous studies in showing that transition does not occur at a particular value of R_x or R_δ. The tests show that a later transition occurs on thicker airfoils, which partly explains the relatively low values of c_{d_0} obtained with the N. A. C. A. 0018 airfoil at zero lift. With increasing lift coefficient and Reynolds Number, the transition point on the upper surface moves toward the stagnation point. The width of the transition region shows no large variation with Reynolds Number.

An attempt to correlate the transition data with profile-drag measurements with the aid of existing data on the skin-friction drag of flat plates proved unsuccessful, indicating that further study is required in order to predict the drag of an airfoil even when the transition is known.

The wind-tunnel measurements of the transition point are at an advantage over flight measurements in that it is possible to determine separately the effects of Reynolds Number and lift coefficient; however, there are serious disadvantages owing to the initial wind-tunnel turbulence. The conclusions of these tests are therefore restricted until projected flight tests for comparison with the full-scale-tunnel measurements have been made.

LANGLEY MEMORIAL AERONAUTICAL LABORATORY,
NATIONAL ADVISORY COMMITTEE FOR AERONAUTICS
LANGLEY FIELD, VA., *May 26, 1938.*

REFERENCES

1. Burgers, J. M.: The Motion of a Fluid in the Boundary Layer along a Plane Smooth Surface. Proc. First Int. Congress for Appl. Mech., Delft, 1924, C. B. Biezeno, J. M. Burgers, ed., J. Waltman (Delft), 1925, pp. 113–128.
2. van der Hegge Zijnen, B. G.: Measurements of the Velocity Distribution in the Boundary Layer along a Plane Surface. Report 6, Aero. Lab. Tech. H. S. Delft, 1924.
3. Dryden, Hugh L.: Air Flow in the Boundary Layer near a Plate. T. R. No. 562, N. A. C. A., 1936.
4. Jones, B. Melvill: Flight Experiments on the Boundary Layer. Jour. Aero. Sci., vol. 5, no. 3, Jan. 1938, pp. 81–94.
5. Platt, Robert C.: Turbulence Factors of N. A. C. A. Wind Tunnels as Determined by Sphere Tests. T. R. No. 558, N. A. C. A., 1936.
6. Goett, Harry J., and Bullivant, W. Kenneth: Tests of N. A. C. A. 0009, 0012, and 0018 Airfoils in the Full-Scale Tunnel. T. R. No. 647, N. A. C. A., 1938.
7. Dryden, H. L., and Kuethe, A. M.: Effect of Turbulence in Wind Tunnel Measurements. T. R. No. 342, N. A. C. A., 1930.

U. S. GOVERNMENT PRINTING OFFICE: 1939

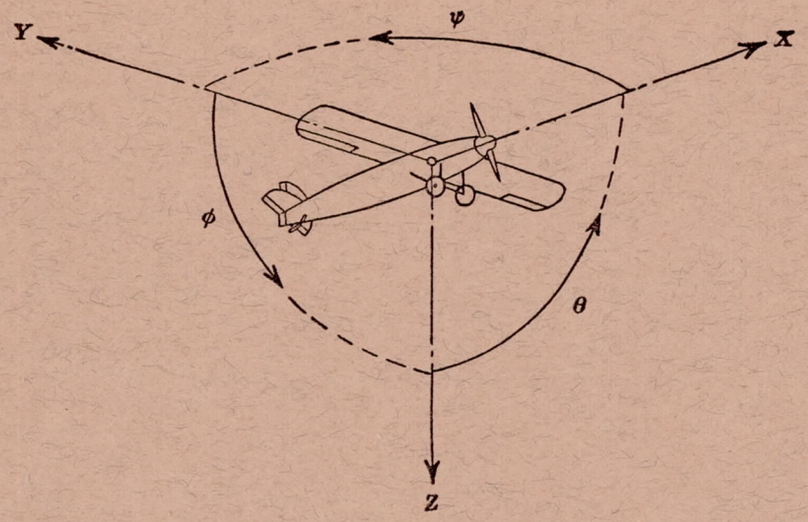

Positive directions of axes and angles (forces and moments) are shown by arrows

Axis		Force (parallel to axis) symbol	Moment about axis			Angle		Velocities	
Designation	Symbol		Designation	Symbol	Positive direction	Designation	Symbol	Linear (component along axis)	Angular
Longitudinal	X	X	Rolling	L	$Y \longrightarrow Z$	Roll	ϕ	u	p
Lateral	Y	Y	Pitching	M	$Z \longrightarrow X$	Pitch	θ	v	q
Normal	Z	Z	Yawing	N	$X \longrightarrow Y$	Yaw	ψ	w	r

Absolute coefficients of moment

$C_l = \frac{L}{qbS}$ (rolling) $\quad C_m = \frac{M}{qcS}$ (pitching) $\quad C_n = \frac{N}{qbS}$ (yawing)

Angle of set of control surface (relative to neutral position), δ. (Indicate surface by proper subscript.)

4. PROPELLER SYMBOLS

D, Diameter

p, Geometric pitch

p/D, Pitch ratio

V', Inflow velocity

V_s, Slipstream velocity

T, Thrust, absolute coefficient $C_T = \frac{T}{\rho n^2 D^4}$

Q, Torque, absolute coefficient $C_Q = \frac{Q}{\rho n^2 D^5}$

P, Power, absolute coefficient $C_P = \frac{P}{\rho n^3 D^5}$

C_s, Speed-power coefficient $= \sqrt[5]{\frac{\rho V^5}{P n^2}}$

η, Efficiency

n, Revolutions per second, r.p.s.

Φ, Effective helix angle $= \tan^{-1}\left(\frac{V}{2\pi r n}\right)$

5. NUMERICAL RELATIONS

1 hp.=76.04 kg-m/s=550 ft-lb./sec.

1 metric horsepower=1.0132 hp.

1 m.p.h.=0.4470 m.p.s.

1 m.p.s.=2.2369 m.p.h.

1 lb.=0.4536 kg.

1 kg=2.2046 lb.

1 mi.=1,609.35 m=5,280 ft.

1 m=3.2808 ft.